MINERALOGICAL MAGAZINE, JUNE 1985, VOL. 49, PP. 413–423

Electron-optical studies of phyllosilicate intergrowths in sedimentary and metamorphic rocks

S. H. WHITE, J. M. HUGGETT*, AND H. F. SHAW

Department of Geology, Imperial College, London SW7, UK

ABSTRACT. The results of a microstructural study by backscattered scanning electron microscopy and a microchemical study using X-ray microprobe analysis of phyllosilicate intergrowths from sandstones, shales, metagreywackes, and low-grade schists are presented. The microstructural study revealed that the intergrowths thicken and become more coherent with metamorphic grade; the intergrowths change from incoherent to coherent in the anchizone. The increasing coherency is mirrored by an increase in the crystallinity indices of the illites/phengites. Chemical analysis of the individual intergrowth phases was difficult in the sediments and no systematic compositional variations were recorded. However, clear compositional trends with increasing metamorphic grade emerged in the phengites from the metagreywackes and schists, but in the chlorites only slight compositional changes were recorded.

KEYWORDS: electron microscopy, electron microprobe analysis, phyllosilicates, illite, phengite, sedimentary rocks, metamorphic rocks.

RECENT electron-optical studies of sedimentary and low-grade metamorphic rocks have revealed the common presence of very fine-scale phyllosilicate intergrowths which cannot be resolved by optical microscopy (White *et al.*, 1984; Huggett, 1984; Pye and Krinsley, 1983; Knipe, 1979, 1981). Although the presence of intergrowths can be detected from selected area diffraction patterns in the TEM (Huggett and White, 1982) it has not been possible to examine, in detail, their morphologies. Consequently it can often be difficult to differentiate the individual phases that compose the intergrowths. This poses problems when chemically characterizing the phases in the intergrowths. The use of back-scattered SEM analysis overcomes these drawbacks as the petrography of the intergrowths can be viewed directly from their atomic number contrast imaging (see White *et al.*, 1984; and fig. 1) and the individual phases that are imaged can then be readily characterized chemically using either an X-ray energy dispersive spectrometer or X-ray wavelength dispersive spectrometers.

A further advantage of back-scattered SEM X-ray chemical microanalysis over TEM X-ray chemical microanalysis is that the analysis of hydrated mineral phases are not normalized to 100%. Although much finer intergrowths can be detected, the effective minimum intergrowth width for X-ray chemical microanalysis in the back-scattered SEM is limited to 2 μm by beam spreading.

The aims of the research described here are to characterize the morphological and mineralogical nature of the phyllosilicate intergrowths that have been observed and to discuss their likely origins. Detailed crystal chemical data are presented and illustrate how processes can now be discussed in terms of compositional variations within individual grains, rather than bulk compositional changes. The presence of these phyllosilicate intergrowths needs to be widely realized as the interpretation of X-ray microprobe analyses of such grains as single phases would be seriously misleading.

Experimental techniques

Specimens of oil shales, sandstones, metagreywackes, and of low-grade metamorphic schists were examined and found to contain various types of phyllosilicate intergrowths. The oil shales studied are the Oil Shales of Carboniferous age from Lothian, Scotland, that have suffered compaction and in some instances deformation producing minor fold structures. The sandstone specimens are fine grained sublithic arenites from the Eagle Sandstone of the Westphalian Coal Measures of the East Midlands, UK. They contain minor amounts of feldspar, mica and chlorite with quartz present as a cementing phase along with authigenic kaolinite, illite, siderite, and Fe-dolomite.

The metagreywackes studied came from a sequence across the prehnite–pumpellyite schist zone from the South Island of New Zealand. Three specimens were

* Present address: BP Petroleum Development Limited, Britannic House, London EC2, UK.

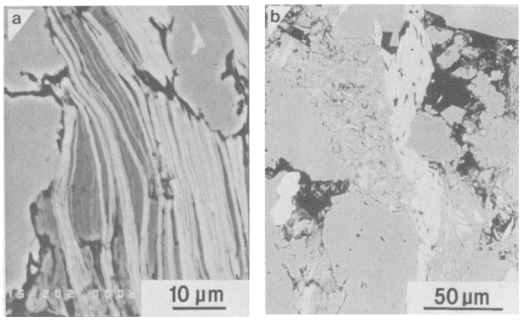

FIG. 1. Backscattered electron micrographs from the Eagle Sandstone. (*a*) A fine-scale incoherent intergrowth between chlorite (light strands) and kaolinite (dark strands) in a detrital chlorite grain. (*b*) Pore-filling authigenic kaolinite with remnant intergrowths of chlorite (light strands).

selected along the Arthurs Pass road through the Southern Alps. Specimen A is from the most easterly outcrops of the zone, specimen C from the westerly outcrops before the greenschist facies schists, and specimen B from the middle area of the traverse. The metamorphic temperature should increase from A to C and this was confirmed by illite crystallinity index measurements (see later). The schists were from the textural subzones 2, 3, and 4 within the chlorite grade of the Haast Schists and also the biotite and biotite–garnet zones of the same schists.

The metagreywackes consist of angular clasts of plagioclase, alkali feldspar, and quartz with abundant detrital biotites and muscovite in a matrix of fine-grained minerals that are difficult to resolve by optical microscopy. The chlorite zone specimens show a metamorphic foliation, with grain size increasing from sub-zones 2 to 4, and have a characteristic greenschist mineralogy of chlorite, epidote, albite, quartz, and phengite with actinolite present in specimens from subzones 3 and 4. The specimens from the biotite zone contain chlorite, biotite, white mica and albite with some almandine and oligoclase appearing and chlorite disappearing in the garnet zone. The schists have suffered a complex, five-phase deformation history (Cooper, 1974) but the specimens examined only show F1, during which the metamorphic foliation was initially developed, the F2 refolding and the F3 crenulations. Peak metamorphic temperatures occurred after F2 and outlasted F3.

All the specimens were examined by the backscattered imaging mode in a JEOL JXA 733 scanning electron microscope/microprobe and analyses made with the X-ray energy dispersive (EDS) spectrometer. The application of the backscattered SEM to petrological studies has been discussed by Lloyd and Hall (1981) and to studies of sedimentary rocks in particular by White *et al.* (1984). Briefly a polished petrological thin section (or for shales a polished block) similar to that used for conventional electron microprobe analysis is employed and given a conducting coating of carbon. In the backscattered imaging mode contrast is due to variations in the mean atomic number of the minerals present, the higher the mean atomic number the brighter the image. The technique allows individual mineral phases to be identified and slight variations in their mineral chemistry to be characterized by EDS. The back-scattered detector can discriminate between phases with average atomic number differences of 0.1 or above. This sets the lower limit for detecting compositional variations in the phyllosilicates and, for example, corresponds to a variation in the K_2O

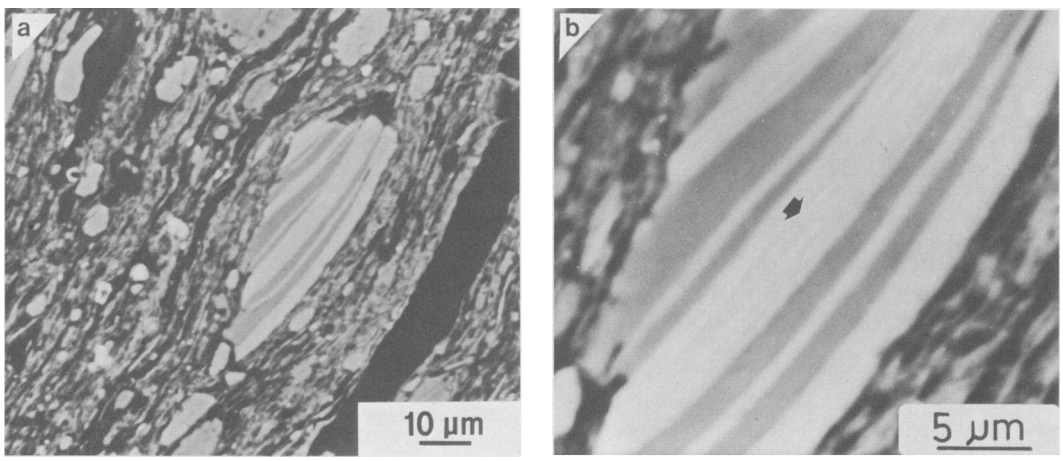

FIG. 2. Backscattered electron micrographs from the Lothian oil shale. (*a*) General microstructure showing a large detrital chlorite (see (*b*) in a fine-grained matrix consisting mainly of incoherently intergrown chlorite and illite. (*b*) Large detrital chlorite grain showing the incoherent intergrowth between chlorite (light phase) and illite (darker phase). Fine-scale intergrowths occur in the area arrowed. Note the variations in contrast in the chlorite intergrowths indicating compositional variations.

content of an illite of 1 wt. % or a 0.5 wt. % variation in the FeO content of a chlorite (White *et al.*, 1984).

Quantitative chemical analyses were performed using an energy dispersive X-ray spectrometer controlled by a Link Specta System. Quantitative mineral analyses were obtained using standard ZAF correction procedures within the Specta software supplied by Link Systems. Cobalt was used as an intermediatory standard. An operating voltage of 15 kV with a current of 5nA was used for both the backscattered imaging and the microchemical analyses. The beam width employed provided an excitation area of about 2 μm diameter and this represents the lower limit for the mineral grain size that can be analysed. In addition to the electron optical studies the crystallinity indices of the illite/muscovite present in the samples was determined by X-ray diffraction analyses of the < 2 μm fractions (Table I).

TABLE I.

Illite crystallinity values of samples studied (Kubler Index)

Sample	Kubler Index (°2θ CoKα)	Classification
Eagle Sandstone	0.45-0.65	Diagenetic
Oil Shale	0.80	Diagenetic
Greywackes		
A	0.35	Anchizone
B	0.28	Anchizone
C	0.23	Epizone
Schist chlorite subzone 2.	0.18	Epizone

Results

In the shales and sandstones examined, intergrowths between illite, chlorite, and kaolinite are commonly found in both detrital and authigenic pore-filling phases and vary in scale from very fine (i.e. 0.25 μm thick) to much broader lamellae several microns wide (figs. 1 and 2). In the Eagle Sandstone, chlorite lamellae often form incoherent (i.e. not in structural continuity) and coherent (i.e. apparently in structural continuity) intergrowths with illite and kaolinite (fig. 1, and see also Huggett, 1984). The intergrowths may take the form of thin lamellae within broader lamellae of a second phase, whilst other lamellae bifurcate or wedge apart lamellae of the different phases. The coherent nature of many of the intergrowths suggests the simultaneous authigenic formation of the phases. The incoherent intergrowths could arise from local displacive growth of one phase within a pre-existing phyllosilicate (Huggett, 1984). Similar intergrowths occurred in the clay size phyllosilicates within pore infills where kaolinite grains have within them mainly incoherent intergrowths of illite and, especially, of chlorite (fig. 1*b*).

The authigenic origin of many of the intergrowths in both detrital grains and pore infills in the sandstone and shale samples is further suggested by their delicate morphologies, but there are others in detrital phyllosilicates that from their robust morphologies suggest a detrital origin (fig. 2). We therefore do not agree with the conclusion of Pye and Krinsley (1983) that in sedimentary rocks phyllosilicate intergrowths are generally authigenic. We suggest that they can be detrital and authigenic in origin. In addition to intergrowths of different phyllosilicates, compositional zoning of the same phyllosilicate phase was also observed. This is well illustrated in the chlorite grains in the Eagle Sandstone and in the oil shale samples examined (figs. 1 and 2).

In the metagreywackes the detrital biotite grains always show chlorite and phengite intergrowths in variable proportions (fig. 3). In fig. 3*b* an example is shown in which the biotite is predominantly replaced by phengite, with closer examination revealing lamellae of chlorite in the phengite. Similarly in fig. 3 there are fine intergrowths of phengite in the chlorite whilst the chlorites also shown fine (< 2 μm) compositional zoning. In contrast to the detrital biotites, the white detrital micas are uniformly phengitic in composition. Although showing compositional zoning, they do not contain intergrowths of different phyllosilicate phases.

Details of the microstructure of the metagreywackes are shown in figs. 4 and 5; these indicate differences between metagreywackes A and B on the one hand and C on the other. A weak foliation is seen in C, as well as extensive alteration of the feldspar clasts and an increase in the grainsize of the pore-filling minerals. Angular clasts of quartz, plagioclase, and alkali feldspars are indented and those adjacent to and within pore spaces have been fluted by pressure solution processes. The microstructure of the pore fills is shown in fig. 4*a*.

Small fluted clasts of detrital minerals are surrounded by small (most are < 2 μm) phengites and chlorites which are incoherently intergrown and which also have associated with them, in the infills, epidotes, and sphenes. In greywacke C, the majority of the phengites and chlorites in the pore infills are wider than 2 μm with some up to 10 μm (fig. 6*b* and *c*) and the intergrowths within the interlocking grains are coherent, similar to that seen in metamorphic rocks. All metagreywackes have pores infilled with intergrowths of Fe and Mg-rich chlorites with the former tending to rim the latter (fig. 4*b*).

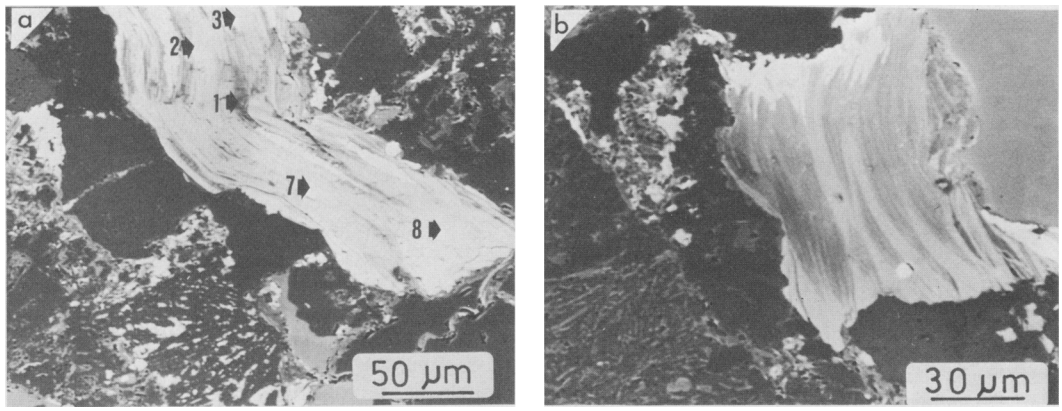

FIG. 3. Backscattered electron micrographs of detrital biotites from metagreywacke B. (*a*) A patchy, incoherent chlorite (intermediate toning), phengite intergrowth (darkest toning), together with sphene (bright toning), replacing a detrital biotite. There are slight tonal variations in the chlorite, indicating compositional heterogeneity in that mineral. Numbers correspond to analysis positions in Table IV which reveal areas of detrital biotites. (*b*) Another example of a chlorite/phengite intergrowth replacing a biotite, also with associated sphene. The relative tonings are the same as in (*a*). In this example more phengite (dark toning) has developed and it has within it wispy incoherent intergrowths of chlorite (intermediate toning).

The metamorphic schists of the chlorite, biotite and garnet zones all exclusively show coherent intergrowths of phengite and chlorite (figs. 6–8). With increasing metamorphism, the phyllosilicate grains tend to increase in size and the widths of the coherent intergrowth lamellae tend to become broader (cf. fig. 8), although narrow (< 2 μm) intergrowths are still encountered. In the schists of the chlorite 3 and 4 subzones, narrow intergrowths of chlorite occur in the phengite-rich zones which are generally depleted in quartz and resemble P domains in slates (White and Johnston, 1981) (fig. 8). In the biotite and garnet zones biotite–muscovite intergrowths are rarely seen and the biotite grains show no evidence of intergrowths.

Microchemical analyses of the phyllosilicates grains are presented in Tables II–V and in figs. 9–11. The data for Eagle Sandstone illites and

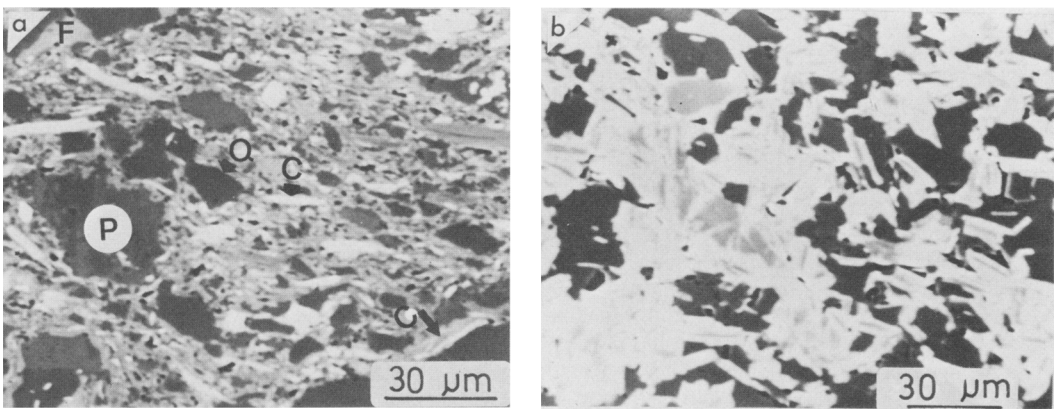

FIG. 4. Backscattered electron micrographs showing microstructures typical of greywackes A and B. (*a*) Details of pore infill. Small bright chlorites (one is labelled C) and phengites (intermediate toning). Incoherent intergrowths can be distinguished in these grains. The very bright blebs are epidotes and sphenes. Plagioclase P, alkali feldspar F, and quartz Q, are marked. These grains were identified by EDS. (*b*) Details of a chlorite/albite (dark areas) infill. Two chlorites are present, an Fe-rich one (bright contrast) rimming and intergrown with a Mg-rich variety (intermediate toning).

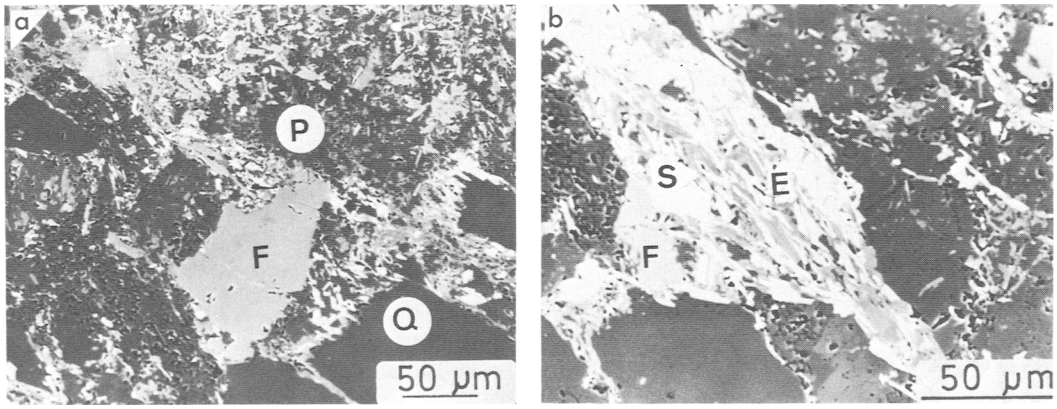

FIG. 5. Backscattered electron micrographs showing microstructures typical of greywacke C. (*a*) General microstructure. Overgrowths have developed on quartz grains Q. Plagioclase grains P, are extensively sericitized whereas the alkali feldspar F, is little affected. A weak metamorphic foliation, not seen in optical micrographs, is apparent. (*b*) Details of a pore infill which consists of intergrown chlorite (light tabular grains) and phengite (grey tabular grains). The large bright grains are sphene (S) and epidote (E). There is also authigenic alkali feldspar (F) present.

TABLE II.

Comparison of major element compositions of new phengites and detrital white mica grains in greywacke A. (Oxide wt.%)

	New phengites (21 analyses)		Detrital white micas (13 analyses)	
	Mean	Std. dev.	Mean	Std. dev.
SiO_2	46.76	0.91	47.19	2.07
Al_2O_3	32.28	2.11	33.33	2.88
FeO	2.35	1.00	1.83	0.85
MgO	1.34	0.71	1.03	0.76
K_2O	9.15	0.57	8.97	0.68

TABLE III.

Comparison of major element compositions between co-existing Fe and Mg-rich chlorites in greywacke C. (Oxide wt.%)

	Fe-rich (16 analyses)		Mg-rich (10 analyses)	
	Mean	Std. dev.	Mean	Std. dev.
SiO_2	26.33	1.52	27.67	1.98
Al_2O_3	20.54	1.29	19.86	1.39
FeO	28.29	2.18	21.13	2.70
MgO	11.86	0.85	18.18	2.53

TABLE IV.

Compositional variations of intergrowths in an originally detrital biotite

See fig.3a for analysis positions

	1	2	3	4	5	6	7	8
SiO_2	46.60	28.20	30.19	29.70	31.92	30.15	34.81	35.12
TiO_2	0.74	2.69	2.55	2.55	2.74	4.27	0.23	1.02
Al_2O_3	30.79	16.63	18.32	18.90	16.52	16.38	21.59	26.99
Cr_2O_3	-	0.64	0.25	0.06	0.07	0.07	0.12	0.06
FeO	5.10	26.44	26.72	27.80	24.05	23.09	19.76	19.72
MnO	0.03	0.51	0.31	0.47	0.25	0.42	0.34	0.06
MgO	1.89	8.82	10.09	10.79	12.58	11.21	10.36	7.95
CaO	-	0.12	0.26	0.14	0.04	1.98	0.27	-
Na_2O	0.29	-	0.12	0.27	0.41	.17	0.46	0.26
K_2O	10.06	3.20	2.80	2.31	4.02	1.73	1.95	3.59
TOTAL	95.50	86.65	91.61	92.99	92.60	89.47	89.89	94.77

TABLE V.

Comparison of major elemental compositions of new chlorites within pore infills and chlorite developed from originally detrital biotites (Oxide wt.%)

	New chlorites (20 analyses)		Chlorites from biotites	
	Mean	Std. dev.	Mean	Std. dev.
SiO_2	27.49	1.91	29.53	1.83
TiO_2	-	-	1.28	0.70
Al_2O_3	20.48	1.17	19.02	1.28
FeO	26.24	2.57	23.78	1.76
MgO	12.15	1.58	12.95	1.62
K_2O	-	-	0.87	0.70

chlorites show a scattered distribution because of the predominance of the < 2 μm intergrowths of the one within the other, and of kaolinite. The white mica compositions in the metagreywackes show a range in compositions from illite/muscovite to phengite, that is the Al_2O_3/SiO_2 and $(FeO+MgO)/SiO_2$ ratios vary markedly while the K_2O/SiO_2 ratio exhibits less variation. Compositions of the metamorphic white micas vary little in the schists within a given zone and plot in the phengitic field, apart from those in the garnet zone which cluster in the muscovite field. They become more phengitic from chlorite 2 and 3 subzones and reverse towards muscovite in the biotite zone. There is a general trend for the K_2O/SiO_2 ratio of the white micas to increase from the sediments to the metagreywackes and schists. Chlorite compositions in the metagreywackes also show a spread in compositions due to variable Fe and Mg contents (fig. 11). The metamorphic chlorites show little compositional variations and cluster in the ripidolite field.

Compositional variations were recorded in the detrital biotite grains in the metagreywackes (Table IV) and confirm the microstructural observations. A zone of K-deficient biotites remains within the chlorite, and the average composition of the chlorites forming from biotite is similar to that of the chlorites in the pores, apart from small amounts of TiO_2 and K_2O (Table IV). The composition of the phengites which developed on the detrital muscovites have the same compositions as the small phengite grains within the pore infills (Table II).

Discussion

Changes in white mica and chlorite compositions with increasing grade. The composition of the white mica became more phengitic on passing from diagenesis through to low-grade metamorphism and is in agreement with other findings (Dunoyer De Segonzac, 1970; Frey, 1978). However, the range in compositions found in the metagreywackes is such that it covers the total range bordering from the illite/muscovite field through to the phengite field. There is no apparent clustering of points in this range. Similarly there is a range in compositions in the chlorites from Mg-rich ripidolites to Fe-rich ripidolites in the metagreywackes but they concentrate towards the Fe-rich ripidolites field on passing into low-grade metamorphism. This trend is also similar to that recorded by Dunoyer De Segonzac (1970) and Frey (1978). The Fe-rich ripidolites rim the Mg-rich, indicating that these ripidolites become more Fe-rich with time. It was not possible to deduce any time relationships for changes in the chemistry of the white micas in the metagreywackes. The range in the compositions of the white micas and chlorites is a likely reflection of the essentially solid state processes by which phyllosilicates alter their compositions (see below). The compositions cluster once into the metamorphic field, when solid state processes are more pronounced, as evidenced by the grain growth of the mineral assemblages.

Intergrowths between phyllosilicate minerals. Intergrowths between illite and chlorite, with or without kaolinite, are common in the sediments

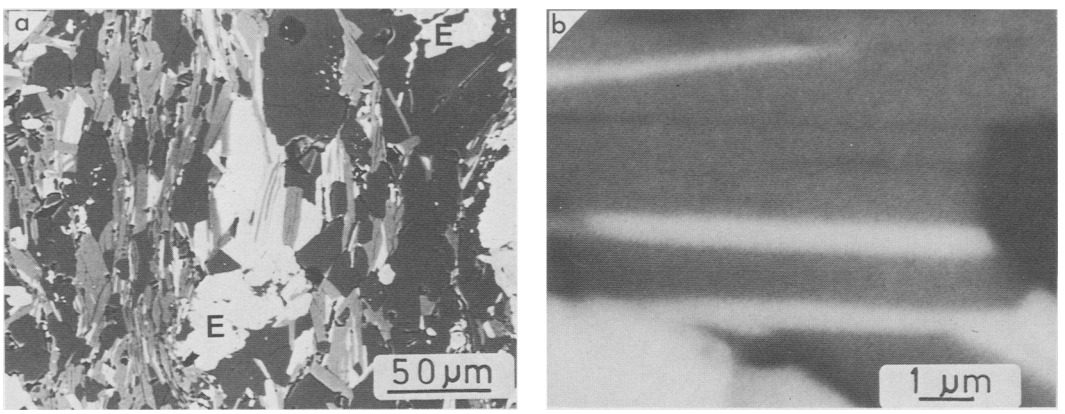

FIG. 6. Backscattered electron micrographs typifying chlorite/phengite intergrowths in the schists from the chlorite sub-zones. The micrographs below are from the chlorite sub-zone 2. (*a*) General microstructure. Intergrowths of chlorite and phengites are generally coarse although narrow growths can be seen. The dark grains are quartz and albite. Epidote grains are marked E. (*b*) Very narrow intergrowths between chlorite (light) and phengite (dark). Note the regular morphology of these coherent intergrowths compared to the wispy intergrowths seen in figs. 1, 2, and 3.

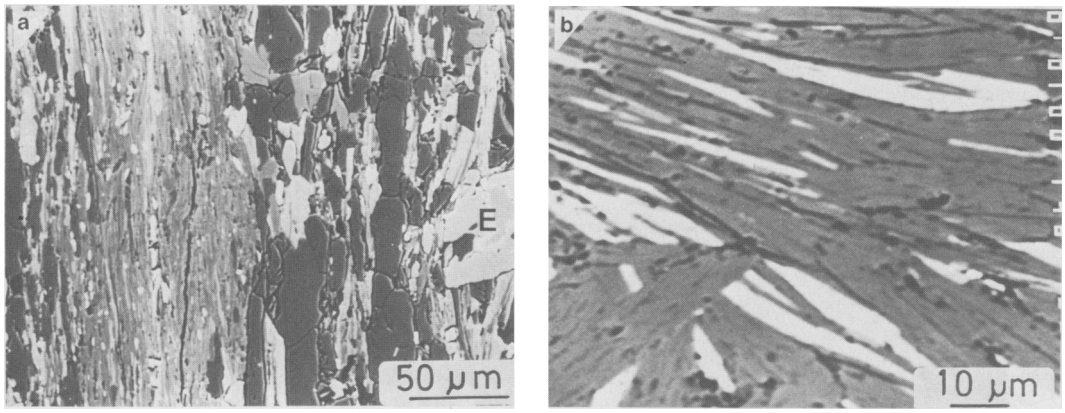

FIG. 7. Phengite-rich domain from chlorite sub-zone 3. (*a*) General microstructure. A zoned epidote is marked E. (*b*) Details of the chlorite intergrowths (bright grains) in the phengites. Note that most of these are narrow and would not be detected in a normal petrological microscope.

studied (see also Huggett, 1984) and between phengite and chlorite in the metagreywackes and schists. In addition, the chlorites in the sediments and metagreywackes have a fine-scale compositional zoning parallel to the basal planes. The zoning is not present in the chlorites from the schists. The phengite–chlorite intergrowths are narrow, have a wispy thread-like appearance and are often incoherent in the sediments and in metagreywackes A and B. They begin to broaden and become more coherent in metagreywacke C and this continues into the schists, although in the latter group fine intergrowths are still encountered but all are coherent.

The morphological progression of the intergrowths from a wispy, incoherent relationship to a euhedral, coherent one mirrors the increase in the illite crystallinity index. At this stage it is not possible to conclude that there is a direct correlation between the two. Both may reflect a more fundamental physico-chemical attribute of the illite–phengite structure and this problem is under investigation. However it is noted that coherent phyllosilicate intergrowths do not give rise to strains (see recent TEM studies by Knipe, 1981; Iijima and Zhu, 1982), whereas incoherent interfaces do, and these strains could cause X-ray line broadening of the type associated with low

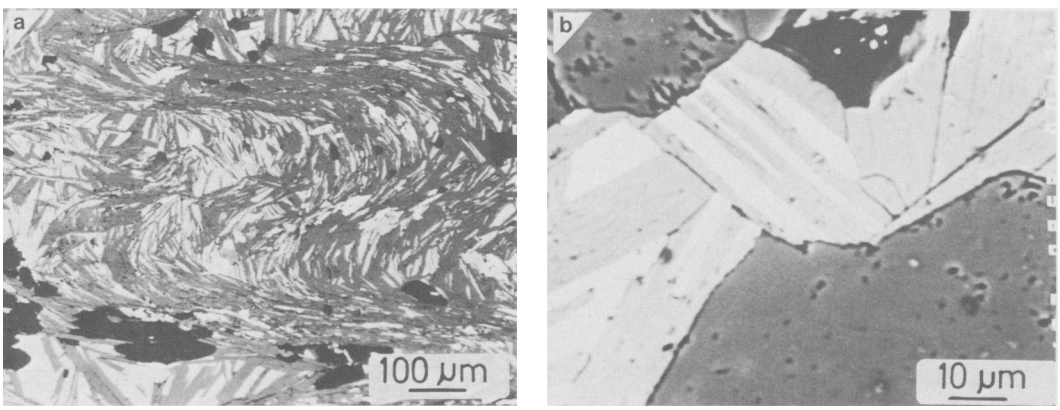

FIG. 8. Backscattered electron micrographs from the biotite sub-zone schists. (*a*) General microstructure. The chlorite phengite intergrowths are crenulated with the limbs of the crenulations being enriched in phengites. The dark grains are quartz and albite. (*b*) Details of the chlorite/phengite intergrowths.

crystallinity indices. The extent of straining associated with incoherent intergrowths is not known and detailed TEM studies are required before any association can be made between the incoherency strains and crystallinity index. It is emphasized that the backscattered electron micrographs indicate that intergrowths are common in the < 2 μm illite and phengite grains.

Crystallochemical changes in originally detrital biotites and white mica. Detrital biotites in the sandstones and shales alter to an authigenic assemblage of illite plus one or both of chlorite and kaolinite whereas in the anchizone the authigenic assemblage is phengite and/or chlorite together with sphene which may form as clusters within or be aligned along the intergrowth interfaces. The relative proportion of each phase varies from grain to grain and there is no set illite/chlorite or phengite/chlorite ratio. The phyllosilicates intergrow both coherently along basal planes or incoherently to form wispy intergrowths. Usually the intergrowths are evenly distributed throughout the detrital biotite but there are instances in which one phase, normally chlorite, is concentrated at the grain margins. Relatively small changes are involved in the biotite to illite or phengite change but our observations indicate that it and the chlorite development should be regarded as a single reaction. In addition kaolinite development should also be included when considering the diagenetic changes. The biotite–chlorite change is common to both the diagenetic and low-grade metamorphic environments and will be regarded as the principal reaction.

The chemical analyses presented in Table IV indicate that the biotite to chlorite change proceeds via an intermediate K-depleted biotite. This reaction based on an idealized biotite composition (no fresh biotite was encountered during analysis) is written below.

$$K_2(Mg_{2.4}Fe^{2+}_{1.6})(Fe^{3+}_{0.6}Ti_{0.1}Al_{1.3})(Si_{5.4}Al_{2.6})O_{20}(OH)_4 \rightarrow$$
(fresh biotite)

$$[K_{0.4}(Mg_{2.4}Fe^{2+}_{1.6})(Fe^{3+}_{0.6}Ti_{0.1}Al_{1.3})(Si_{5.4}Al_{2.6})O_{20}(OH)_4] + 1.6K^+$$
(weathered biotite)

No unique reaction described the weathered biotite to chlorite change. A reaction based on 1 weathered biotite to 1 chlorite is:

$$1\text{ w. biotite} + 12\,H_2O + 1.6\,Mg^{2+} + 2.9\,Fe^{2+/3+} + 0.17\,Ti^{4+} + 0.8\,Si^{4+} + 0.7\,Al^{3+} \rightarrow K_{0.2}(Mg_{4.0}Fe^{2+/3+}_{4.1}Al_{2.8}Ti^{4+}_{0.2})(Si_{6.2}Al_{1.8})O_{20}(OH)_{16} + 0.2K^+ + 12H^+ \quad (1)$$

(The chlorite composition is based on the analysis given in Table V).

However, the above reaction consumes Al^{3+} and Si^{4+} and does not explain the development of chlorite/kaolinite/illite intergrowths. These can be accommodated if 2 weathered biotite → 1 chlorite which then releases the cations necessary for the growth of kaolinite and illite.

$$2\text{ w. biotite} + 8\,H_2O \rightarrow 1\text{ chlorite} + 4.6\,Si^{4+} + 3.2\,Al^{3+} + 0.8\,Mg^{2+} + 0.3\,Fe^{2+/3+} + 0.6K^+ + 8H^+ \quad (2)$$

In both reactions 1 and 2, Al^{3+} is a mobile ion

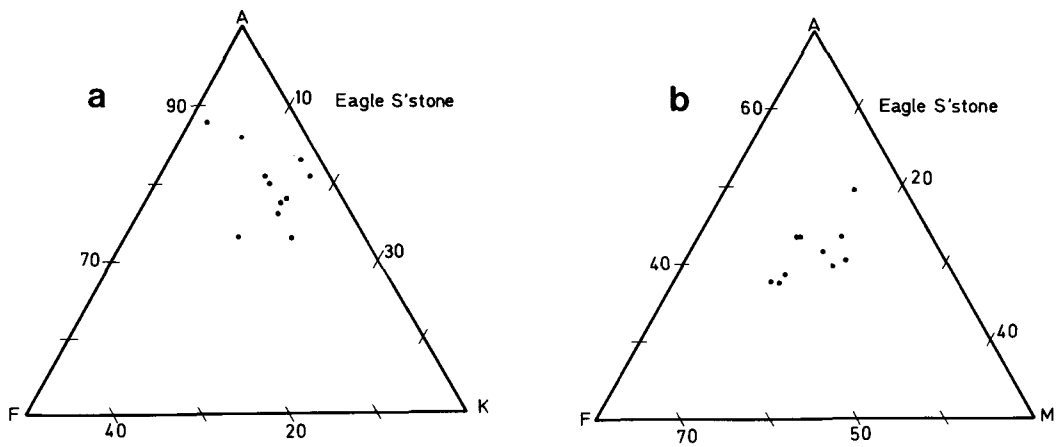

FIG. 9. Illite and chlorite compositions for the Eagle Sandstone plotted on (*a*) AFK diagrams (where A = Al_2O_3/SiO_2, F = $(FeO + MgO/SIO_2$, K = K_2O/SiO_2, and A + F + K = 100) and (*b*) AFM diagrams (where A = Al_2O_3/SiO_2, F = FeO/SiO_2, M = MgO/SiO_2, and A + F + M = 100) respectively.

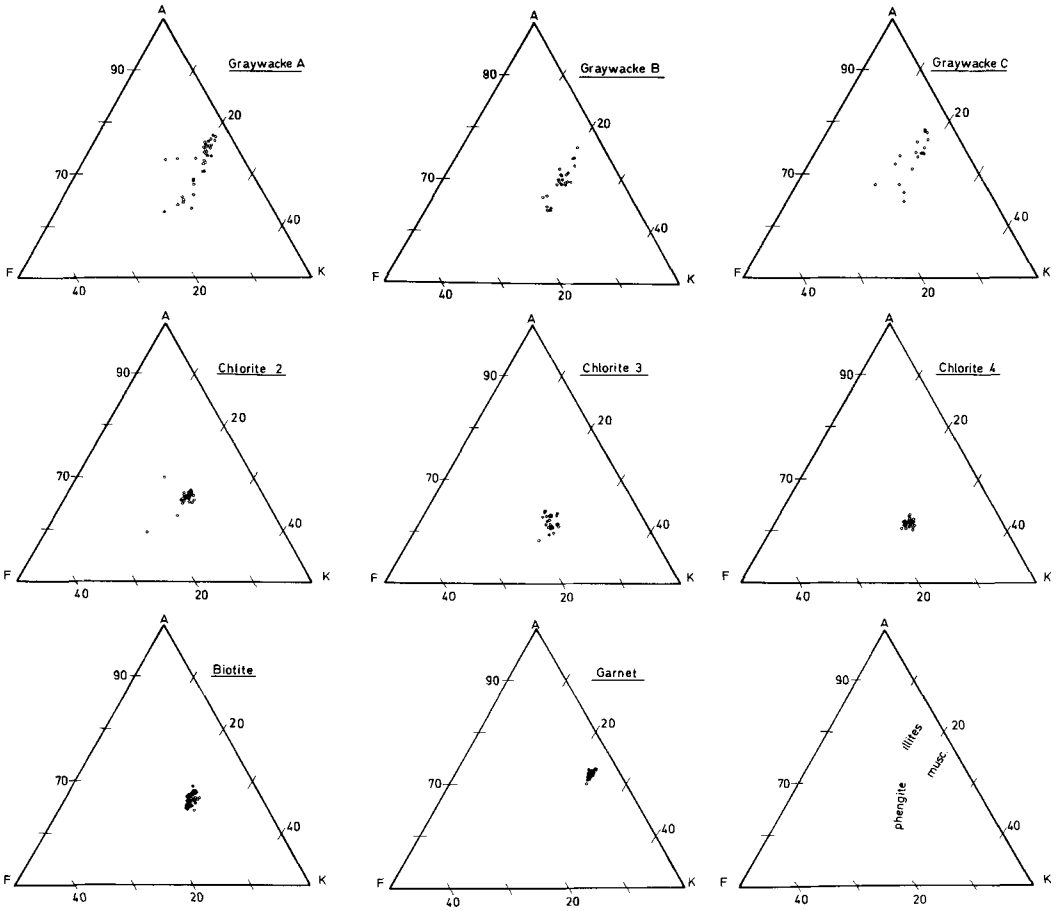

FIG. 10. Compositions of phengites in the metagreywackes and schists plotted on AFK diagrams. A plot showing the compositional fields of illite, phengite, and muscovite is included.

which is doubted (Velde, 1983). A reaction based on constant Al^{3+} is:

$$1.17\,\text{w. biotite} + 1.2\,Mg^{2+} + 1.5\,Fe^{2+/3+} + 0.1\,Si^{4+} + 11.3\,H_2O \rightarrow 1\,\text{chlorite} + 11.3\,H^{+} \quad (3)$$

Reaction 2 best describes the phyllosilicate intergrowths seen in the Eagle Sandstone. Either of reactions 1 or 3 would explain those in the metagreywackes. However, both require that one zone of biotite alters to phengite whilst another adjacent zone alters to chlorite. Neither reaction 1 or 3 describes the total breakdown of biotite; however, reaction 2 does. The lack of any indication of a set phengite (or illite) to chlorite ratio indicates that there is an exchange of the above mobile elements with the environment outside the grain. From this, it can be seen that the above reactions are of limited value in summarizing specific chemical processes that occur during diagenesis and low-grade metamorphism. They are critically dependent upon assumptions made and it is possible to cover any set of assumptions by a given reaction.

The mechanism of the biotite–chlorite reaction has been studied by Ferry (1979) and by Veblen and Ferry (1983). As a result of high resolution TEM study, they concluded that chlorite forms from biotite by the formation of a brucite-like layer by the removal of the tetrahedral sheets of a TOT biotite layer. The reaction via this process leads to a volume decrease of one fifth. There is no evidence of a shrinkage around replaced detrital biotites in our backscattered electron micrographs and it is suggested that any volume decrease is taken up internally by sphene or by the development of other minerals, such as pyrite. The process outlined by

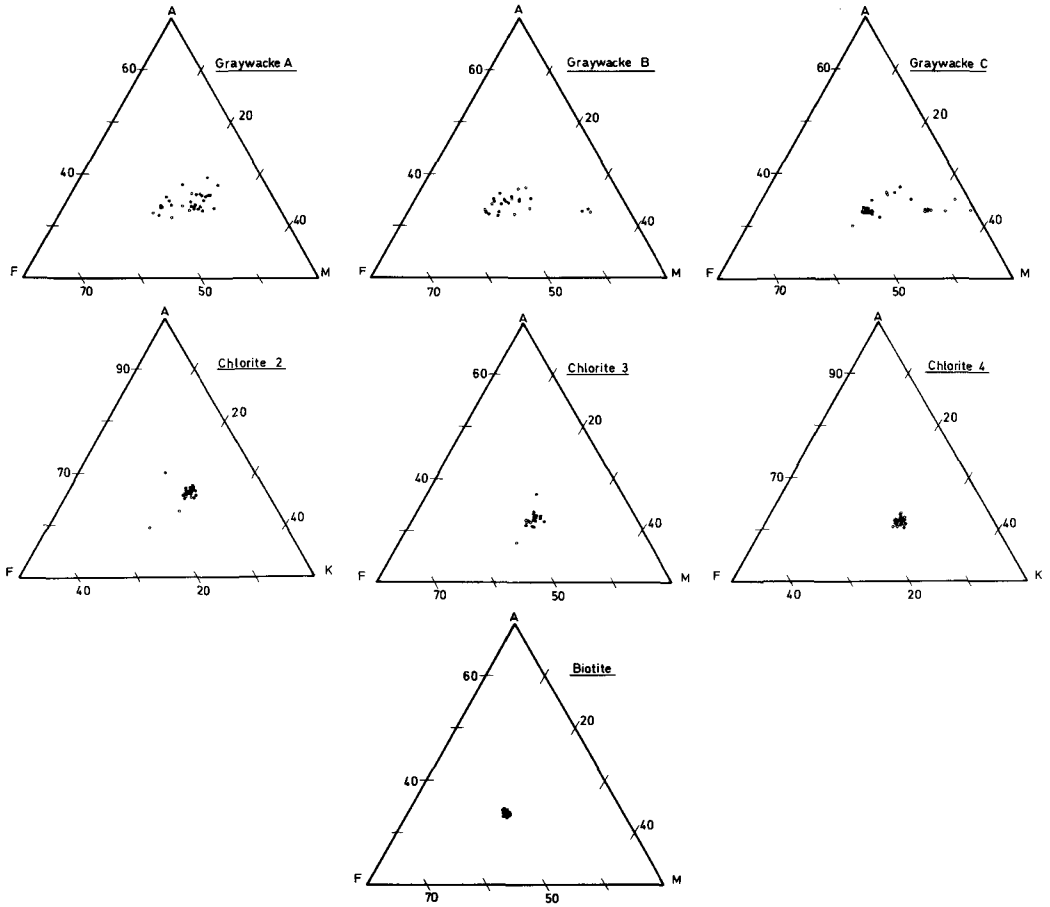

FIG. 11. Compositions of chlorites in the metagreywackes and schists plotted on AFM diagrams.

Veblen and Ferry (1983) is dominantly a solid-state change and it will be governed by the solid-state diffusion of the involved ions, including local redistribution of Al^{3+} and Si^{4+} which are regarded as slow moving species. The slowness of solid-state reactions at low temperatures would account for the persistence of detrital biotite in the diagenetic record and its incomplete replacement by a stable illite (or phengite)-chlorite assemblage based on the biotite lattice. The backscattered micrographs did not reveal any evidence that the biotite participates in a solution-type reaction.

Conclusions

The following conclusions are arrived at for the rocks studied.

1. Backscattered scanning electron microscopy is a powerful technique when studying intergrowths in phyllosilicates. It can also reveal compositional zoning in a given intergrowth phase.

2. Intergrowths change from incoherent to coherent with increasing grade with most change occurring at the top of the anchizone.

3. Crystallinity indices appear to mirror changes in the coherency of intergrowths.

4. Detrital biotites and muscovites change composition by an essentially solid-state process during diagenesis and very low-grade metamorphism.

5. White micas become more phengitic and their K_2O/SiO_2 increases during low-grade metamorphism although in the anchizone there is a spread in compositions in the specimens studied.

6. There is a range in composition in the chlorites from Mg-rich to Fe-rich ripidolites up to the anchizone in the metagreywackes but compositions concentrate in the Fe-rich ripidolite field in the schists.

Acknowledgements. Messrs P. R. Grant and P. Suddaby are thanked for automating the analytical facilities on the JXA 733 and Mr D. Giddens for technical assistance with the SEM. S.H.W. acknowledges support from NERC Grant GR3/3848.

REFERENCES

Cooper, A. F. (1974) *N.Z. J. Geol. Geophys.* **17,** 855–80.
Dunoyer De Segonzac, G. (1970) *Sedimentology*, **15,** 281–346.
Ferry, J. M. (1979) *Contrib. Mineral. Petrol.* **68,** 125–39.
Frey, M. (1978) *J. Petrol.* **19,** 93–135.
Huggett, J. M. (1984) *Sediment. Geol.* **40,** 233–47.
——and White, S. H. (1982) *Clays Clay Minerals*, **30,** 232–6.
Iijima, S., and Zhu, J. (1982) *Am. Mineral.* **67,** 1195–205.
Knipe, R. J. (1979) *Bull. Mineral.* **102,** 206–9.
——(1981) *Tectonophysics*, **78,** 249–72.
Lloyd, M. G., and Hall, G. E. (1981) *Am. Mineral.* **66,** 362–8.
Pye, K., and Krinsley, D. H. (1983) *Nature*, **304,** 618–20.
Veblen, D. R., and Ferry, J. M. (1983) *Am. Mineral.* **68,** 1160–8.
Velde, B. (1983) In *Sediment Diagenesis* (A. Parker and B. W. Sellwood, eds.) NATO AST Series C: Mathematical and Physical Series W/115 215–68. D. Reidel Holland.
White, S. H., and Johnston, D. C. (1981) *J. Struct. Geol.* **3,** 279–90.
——Shaw, H. F., and Huggett, J. M. (1984) *J. Sediment. Petrol.* **54,** 487–94.

[*Manuscript received 15 May 1984; revised 4 September 1984*]